Design imperfections for steel beam lateral torsional buckling

DESIGN IMPERFECTIONS FOR STEEL BEAM LATERAL TORSIONAL BUCKLING

H.H. Snijder, R.P. van der Aa, H. Hofmeyer, B.W.E.M. van Hove

Eindhoven University of Technology (TU/e), Department of the Built Environment, The Netherlands

Abstract: To perform geometrically and materially nonlinear analyses including imperfections for steel beam lateral torsional buckling, the size and shape of the geometric imperfection can be obtained from EN 1993-1-1. The shape is prescribed as an initial bow along the weak axis of the section, excluding torsion of the cross-section. The shape of the imperfection can alternatively be taken equal to the lateral torsional buckling mode, including torsion. Several tables and formulas exist to determine the size of the imperfection. Different imperfection approaches were applied in finite element simulations to evaluate the lateral torsional nonlinear buckling resistances and to compare them to the results obtained with design rules.

1. Introduction

Eurocode 3 provides design rules for the assessment of lateral torsional buckling (LTB) in clause 6.3.2 of EN 1993-1-1 [1]. Alternatively, the code allows LTB to be assessed by performing Geometrically and Materially Nonlinear Analyses with Imperfections of beams. For carrying out such GMNIA calculations, the size and shape of the equivalent geometric imperfection is given in clause 5.3.4(3) of EN 1993-1-1. The shape is prescribed as an equivalent initial bow of the weak axis of the profile considered, excluding torsion of the cross-section. This comes down to the weak axis flexural buckling (FB) mode. The size is prescribed as $ke_{0,d}$ where k is a factor having as recommended value $k = 0.5$ and $e_{0,d}$ is the initial local bow imperfection given in Table 5.1 of EN 1993-1-1. As an alternative, the initial local bow imperfection $e_{0,d}$ can be based on eq. (5.10) of EN 1993-1-1:

$$e_{0,d} = \alpha\left(\bar{\lambda} - 0.2\right)\frac{M_{Rk}}{N_{Rk}} \tag{1}$$

where α is the imperfection factor according to Table 6.1 of EN 1993-1-1, $\bar{\lambda}$ is the non-dimensional slenderness for weak axis buckling, M_{Rk} is the characteristic moment resistance,

and N_{Rk} is the characteristic normal force resistance. In case of class 1 and 2 cross-sections $M_{Rk} = M_{pl}$ and $N_{Rk} = N_{pl}$ where M_{pl} is the plastic moment resistance of the cross-section and N_{pl} is its plastic normal force resistance.

In line with clause 5.3.2(11) of EN 1993-1-1, the shape of the imperfection can also be taken according to the LTB mode, including torsion of the cross-section. For the size of the imperfection, Eq. (1) can be used. However, for the next generation of Eurocodes, new LTB design rules [2,3] have been derived as an alternative to those of the current EN 1993-1-1. Using these new LTB design rules and their derivation, a formula has been obtained which, for an LTB mode, describes explicitly the imperfection size:

$$e_{0,d} = \alpha_{LT}\left(\bar{\lambda} - 0.2\right)\frac{M_{Rk}}{N_{Rk}} \tag{2}$$

where α_{LT} is the imperfection factor according to Table 1. In Table 1 h is the section height, b is the section width and $W_{el,y}$ respectively $W_{el,z}$ are the strong and weak axis section modulus.

The three different imperfection approaches for LTB as shown in Table 2 have been considered in this paper.

Table 1: Imperfection factors for Eq. (2)

Cross-section	Limits	α_{LT}
Rolled I-section	$h/b > 1.2$	$0.12\sqrt{W_{el,y}/W_{el,z}} \le 0.34$
	$h/b \le 1.2$	$0.16\sqrt{W_{el,y}/W_{el,z}} \le 0.49$

Table 2: Three imperfection approaches

Approach	Imperfection shape	Imperfection size
1	Weak axis FB mode, excluding torsion	Eq. (1)
2	LTB mode, including torsion	Eq. (1)
3	LTB mode, including torsion	Eq. (2)

A finite element model for LTB was developed and verified using several other models in literature. With that model, the different approaches for imperfection shape and size were applied to evaluate the LTB resistances. Subsequently, these LTB resistances were compared with the LTB resistances according to the appropriate design rules. For the approaches 1 and 2 the design rules according to the clauses 6.3.2.1 and 6.3.2.2 for the so called 'general case' were used as reference while for approach 3 the newly developed design rules according to [2,3] was used. This paper is based on research work as reported in [4].

2. Scope

The imperfection study in this paper is carried out for hot-rolled class 1 and 2 IPE, HEA, and HEB sections. However, the fillet radius between web and flanges is neglected; therefore the sections are denoted by adding an asterisk: e.g. IPE* sections. The section properties have been modified accordingly. Three load cases have been considered as indicated in Fig. 1.

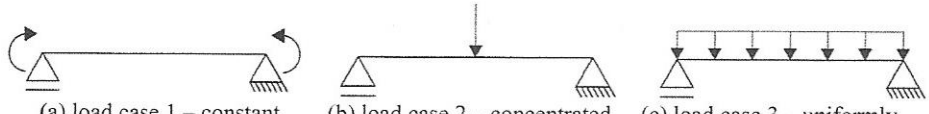

(a) load case 1 – constant bending moment

(b) load case 2 – concentrated load

(c) load case 3 – uniformly distributed load

Fig. 1: Three load cases (LC) considered

3. Finite element model

For the finite element model, so-called "S8R" Mindlin-Reissner elements are used within Abaqus. These are quadrilateral eight node shell elements with six degrees of freedom per node, four integration points in surface direction, and five integration points in thickness direction. The elements require a regular mesh and are suitable for thick shell applications. Eight elements over the width of the flanges and 16 elements over the height of the web are applied. A bilinear stress-strain diagram, neglecting strain hardening, is used with yield stress f_y = 235 N/mm^2, Young's modulus E = 2.1 x 10^5 N/mm^2, and Poisson's ratio 0.3. The Von Mises yield criterion was applied. With respect to the boundary conditions, Fig. 2 shows the end fork conditions of the beam.

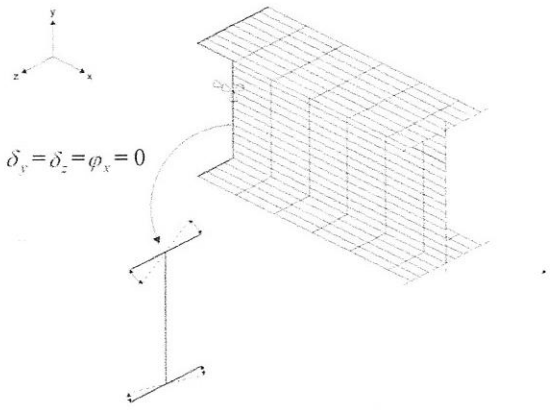

Fig. 2: End fork conditions of the beam

Distortion of the end cross-section is prevented by applying kinematic coupling constraints. This results in an in-plane stiff cross-section (as δ_y and δ_z of all nodes are coupled), which cannot rotate along the beam axis (as $\varphi_x = 0$ for all nodes), but warping is still allowed. Since beam geometry, load cases, imperfection shapes, and failure modes are symmetrical, only half the beam is modelled applying symmetry conditions $\delta_x = 0$, $\varphi_y = 0$, and $\varphi_z = 0$.

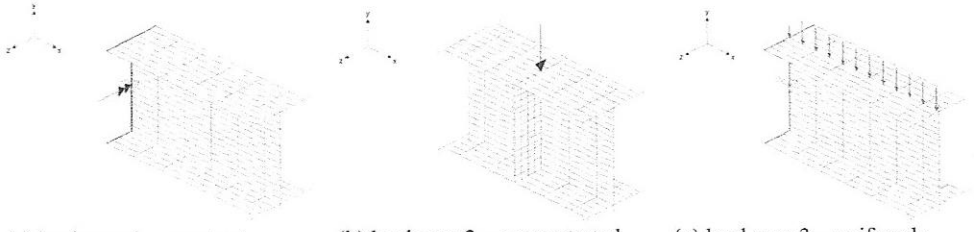

(a) load case 1 – constant bending moment

(b) load case 2 – concentrated load

(c) load case 3 – uniformly distributed load

Fig. 3: Application of loads

Loads are applied as shown in Fig. 3. For the GMNIA, two types of imperfection shapes, i.e. the weak axis FB mode excluding torsion and the LTB mode including torsion are applied after performing the relevant linear buckling analysis (LBA). In Fig. 4 these shapes are shown in the cross-section at mid-span of the beam. For the LTB mode the size of the imperfection is measured at the heart of the top flange.

As a validation of the finite element model, its results obtained from GMNIA calculations were compared with numerical results of [2, 5] and were found to be in good agreement [4].

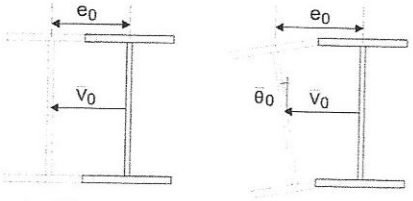

(a) FB mode (b) LTB mode

Fig. 4: Two imperfection shapes at cross-section halfway the beam

4. Simulation and comparison procedure

The comparison of simulations with the finite element method (FEM) and EN 1993-1-1 design rule results is illustrated for an IPE240* section with a length of 3400 mm for load case 1 (constant bending moment) and imperfection approach 2: LTB shape and size of the imperfection according to Eq. (1). First an LBA is performed resulting in an elastic critical bending moment M_{cr} = 84.1 kNm. See Fig. 5 for the corresponding buckling mode which is also used for the shape of the imperfection.

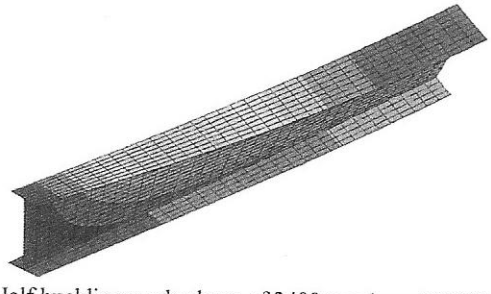

Fig. 5: Half buckling mode shape of 3400 mm long IPE240* beam

The plastic resistance can be calculated as $M_{pl} = W_{pl,y} \cdot f_y = 353.9 \cdot 103 \cdot 235 \cdot 10\text{-}6 = 83.0$ kNm. The non-dimensional slenderness then becomes:

$$\bar{\lambda}_{LT,FEM} = \sqrt{\frac{M_{pl}}{M_{cr}}} = \sqrt{\frac{83.0}{84.1}} = 0.99$$

First the non-dimensional slenderness $\bar{\lambda}$ for weak axis buckling needs to be determined using the elastic critical force for weak axis buckling $N_{cr,z}$:

$$N_{cr,z} = \frac{\pi^2 EI_z}{L_{cr,z}^2} = \frac{\pi^2 \cdot 2.1 \cdot 10^5 \cdot 282.7 \cdot 10^4}{3400^2} = 506.9 \cdot 10^3 \text{ N}$$

$$\bar{\lambda} = \sqrt{\frac{Af_y}{N_{cr,z}}} = \sqrt{\frac{3779 \cdot 235}{506.9 \cdot 10^3}} = 1.32$$

In these calculations I_z is the weak axis second moment of area, $L_{cr,z}$ is the buckling length for weak axis buckling and A is the area of the cross-section. Since $h/b = 240/120 = 2 > 1.2$ and the flange thickness t_f = 9.8 mm is smaller than 40 mm, buckling curve 'b' applies for weak axis buckling according to Table 6.2 of EN 1993-1-1 and the imperfection factor α =

0.34 according to Table 6.1 of EN 1993-1-1. The imperfection size is then determined using Eq. (1):

$$e_{0,d} = \alpha\left(\bar{\lambda} - 0.2\right)\frac{M_{Rk}}{N_{Rk}} = \alpha\left(\bar{\lambda} - 0.2\right)\frac{W_{pl,z}}{A} = 0.34\left(1.32 - 0.2\right)\frac{72772}{3779} = 7.33\,\text{mm}$$

With $k = 0.5$ the final imperfection size becomes: 3.67 mm. With this imperfection size and the imperfection shape of Fig. 5, a GMNIA is performed, for which load-displacement curves are shown in Fig. 6.

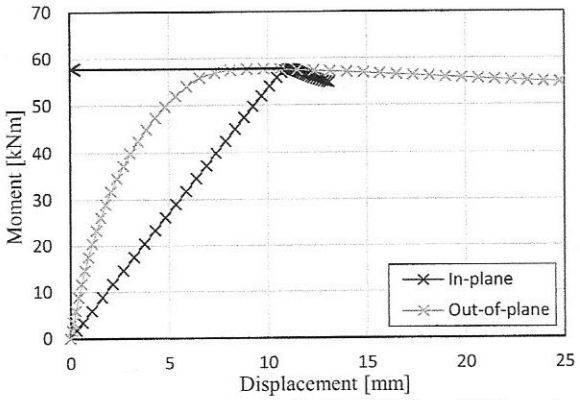

Fig. 6: Load-displacement diagram obtained with GMNIA for a 3400 mm long IPE240* beam

The ultimate load is reached at M_R = 57.6 kNm. The reduction factor can then be calculated as:

$$\chi_{LT,FEM} = \frac{M_R}{M_{pl}} = \frac{57.6}{83.0} = 0.694$$

The combination of $\bar{\lambda}_{LT,FEM} = 0.99$ and $\chi_{LT,FEM} = 0.694$ is compared with the current lateral torsional buckling curve of clause 6.3.2.2 of EN 1993-1-1 as shown in Fig. 7 (black arrows). More results for other non-dimensional slendernesses (beam lengths) and other load cases are

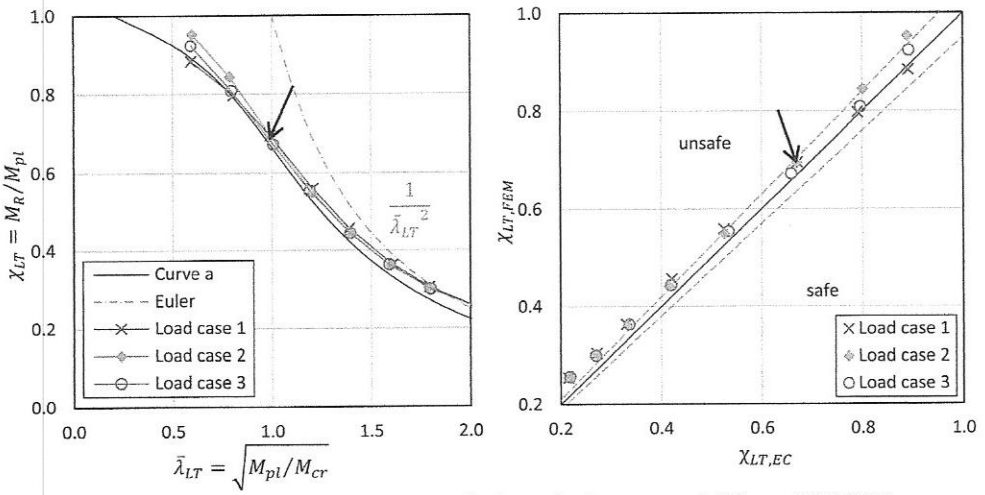

Fig. 7: Comparison of $\chi_{LT,FEM}$ with $\chi_{LT,EC}$ for imperfection approach 2 for an IPE240* beam

also included in Fig. 7. In the left part of Fig. 7 a direct comparison is made between the FEM results and buckling curve of EN 1993-1-1. FEM results above the buckling curve are on the unsafe side, i.e. they are calculated using a too small imperfection size so that $k > 0.5$ should have been chosen. In the right part the reduction factors calculated by FEM are compared with those calculated with EN 1993-1-1, Eurocode 3 (EC3). The diagonal black line represents a perfect match between both reduction factors. If $\chi_{LT,FEM} > \chi_{LT,EC}$ then the FEM results are on the unsafe side. The two dashed lines represent a 5% over- or underestimation.

5. Results

5.1 Imperfection approach 1: weak axis FB mode with Eq. (1) size

The results for imperfection approach 1, with the imperfection shape based on the weak axis FB mode and the imperfection size determined with Eq. (1), are shown in Fig. 8 for an IPE600* beam. Similar results were obtained for IPE240* and HEA300* beams [4].

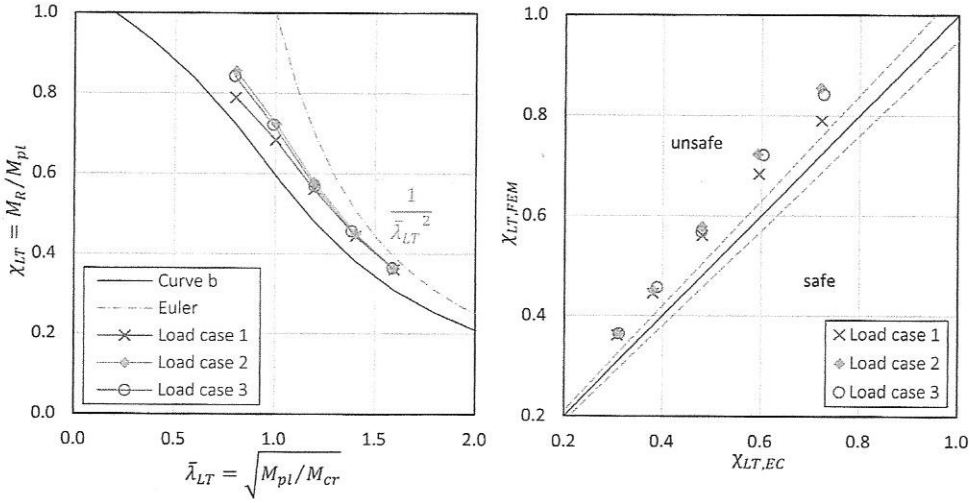

Fig. 8: Comparison of $\chi_{LT,FEM}$ with $\chi_{LT,EC}$ for imperfection approach 1 for an IPE600* beam

As can be seen, load case 2 (concentrated load) gives the largest discrepancies between FEM and EC3 results. All FEM results are largely on the unsafe side of EC3 results meaning that $k = 0.5$ is a far too small value. Therefore, it was decided to determine the k-value more accurately, such that the FEM results are within the 5% limits. The analyses concentrated on load case 2 and on relative slenderness 0.9 where the influence of imperfections is substantial. Fig. 9 shows for IPE beams the required k-values to get $\chi_{LT,FEM}$ to the target value $\chi_{LT,EC}$ as a function of I_y/I_z, where I_y is the strong axis second moment of area. These k-values range from 2.4 to 1.1 and are summarized in Table 3, 3rd column. In a similar way required k-values for HEA beams were obtained [4], also summarized in Table 3.

5.2 Imperfection approach 2: LTB mode with Eq. (1) size

Fig. 7 shows the results for an IPE240* beam for imperfection approach 2, with the imperfection shape based on the LTB mode, and the imperfection size determined with Eq. (1). Similar

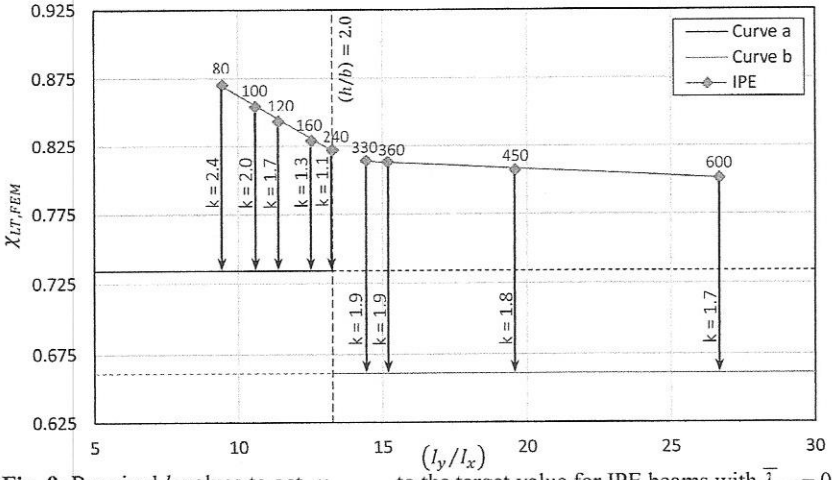

Fig. 9: Required k-values to get $\chi_{LT,FEM}$ to the target value for IPE beams with $\bar{\lambda}_{LT} = 0.9$

Table 3: Required k-values for rolled sections

Section	Limits	Imperfection approach 1	Imperfection approach 2
IPE	$h/b \le 2.0$	$k = -0.34\frac{I_y}{I_z} + 5.60$	$k = -0.13\frac{I_y}{I_z} + 2.44$
	$h/b > 2.0$	$k = -0.017\frac{I_y}{I_z} + 2.15$	$k = -0.017\frac{I_y}{I_z} + 1.44$
HEA	$h/b \le 1.0$	$k = -6.90\frac{I_y}{I_z} + 20.40$	$k = -1.69\frac{I_y}{I_z} + 5.39$
	$1.0 < h/b \le 1.2$	$k = -0.11\frac{I_y}{I_z} + 1.65$	$k = -0.11\frac{I_y}{I_z} + 1.05$
	$1.2 < h/b \le 2.0$	$k = -0.041\frac{I_y}{I_z} + 1.70$	$k = -0.027\frac{I_y}{I_z} + 0.94$
	$h/b > 2.0$	$k = -0.008\frac{I_y}{I_z} + 2.20$	$k = -0.008\frac{I_y}{I_z} + 1.21$

results were obtained for IPE600* and HEA300* beams [4]. In a similar way as described in section 5.1, required k-values were obtained [4], see Table 3, last column. The required k-values for IPE beams range now from 1.2 to 0.7 [4], still substantially greater than 0.5, but far better than for imperfection approach 1 when neglecting torsion, see Fig. 9.

5.3 Imperfection approach 3: LTB mode with Eq. (2) size

Fig. 10 shows the results for IPE240* and HEA300* beams for imperfection approach 3, with the imperfection shape based on the LTB mode, and the imperfection size determined by Eq. (2). For IPE240* beams, all results are satisfactory below the 5% upper limit. For HEA300* beams with $h/b \le 1.2$, the results are close to or even slightly above the 5% upper limit. More beams have been investigated to find similar results [4]. It can be concluded that this imperfection approach, as perhaps may have been expected, leads to consistent results, with the additional benefit that no k-value is needed.

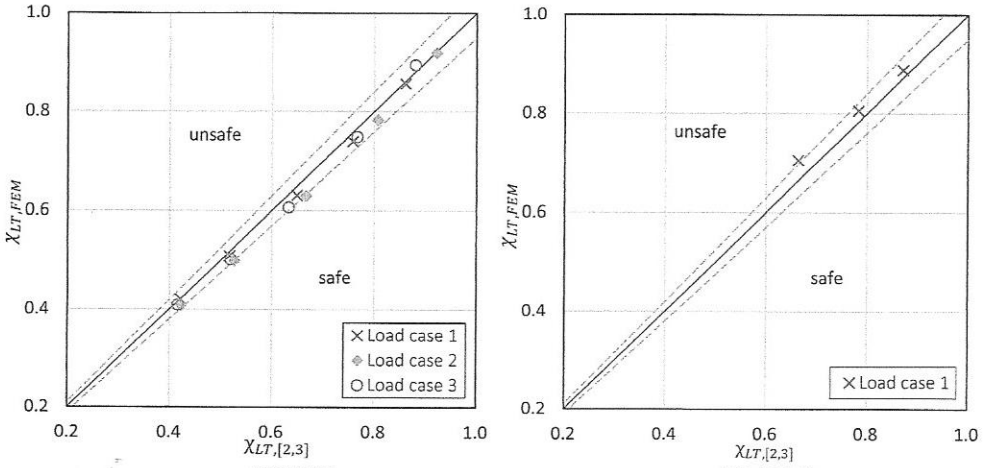

Fig. 10: Comparison of $\chi_{LT,FEM}$ with $\chi_{LT,[2,3]}$ for imperfection approach 3

onclusions

ıree different imperfection approaches were studied to be used in GMNIA calculations for LTB of beams in bending. It is shown that imperfection approach 1, using the FB buckling mode as imperfection shape and Eq. (1) for obtaining the imperfection size, requires k-values far greater than the recommended value $k = 0.5$ in cl. 5.3.4(3) of EN 1993-1-1. Also imperfection approach 2, using the LTB buckling mode as imperfection shape and Eq. (1) for the imperfection size, requires k-values substantially greater than $k = 0.5$, the greatest value being 1.2, indicating that this approach is far better than imperfection approach 1. Consistent results were obtained for imperfection approach 3, using the LTB buckling mode as imperfection shape and Eq. (2) for the imperfection size. This imperfection approach does not need a k-value and is advised to be used in the next version of EN 1993-1-1.

References

[1] EN 1993-1-1. *Eurocode 3: Design of steel structures- part 1-1: General rules and rules for buildings*, Brussels, 2011.

[2] Taras A, Greiner R, Unterweger H. *Proposal for amended rules for member buckling and semi-compact cross-section design*, Doc. CEN-TC250-SC3_N1898, 2013.

[3] Taras A. *Contribution to the development of consistent stability design rules for steel members*, PhD thesis, Graz University of Technology, Graz, Austria, 2010.

[4] Aa RP van der. *Numerical assessment of the design imperfections for steel beam lateral torsional buckling*, Master thesis, report 2015.96, Eindhoven University of Technology, Eindhoven, Dept. of the Built Environment, Structural Design, The Netherlands, 2015.

[5] Bruins RHJ. *Lateral torsional buckling of laterally restrained steel beams*, Master thesis, report 2007.7, Eindhoven University of Technology, Dept. of the Built Environment, Structural Design, Eindhoven 2007.

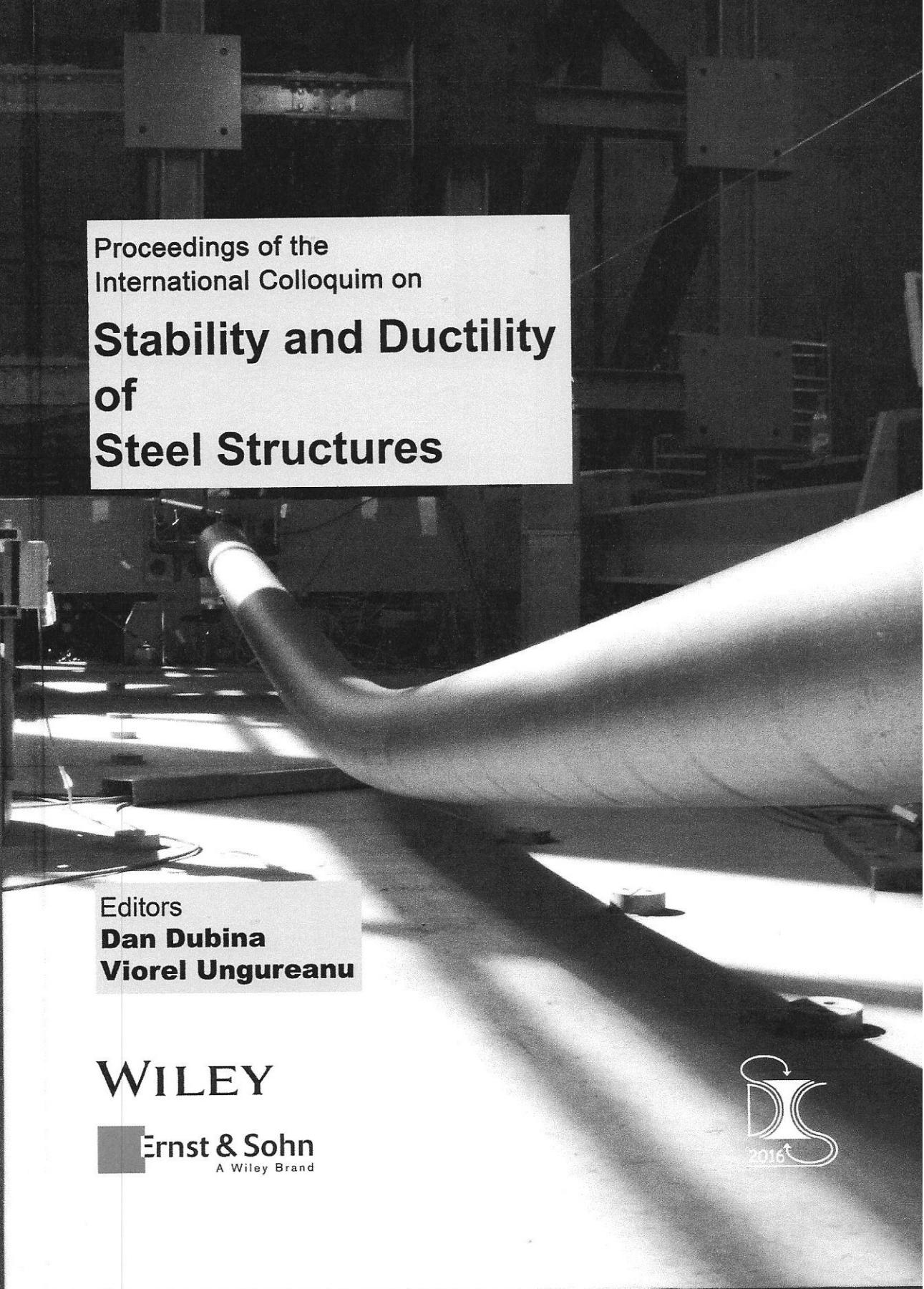

Proceedings of the
International Colloquim on

Stability and Ductility of Steel Structures

Editors
Dan Dubina
Viorel Ungureanu

WILEY

Ernst & Sohn
A Wiley Brand

2016

SDSS'2016

The International Colloquium on Stability and Ductility of Steel Structures

30 May – 01 June 2016, Timisoara, Romania

Proceeding of the conference edited by: Dan Dubina and Viorel Ungureanu

Published by:
ECCS – European Convention for Constructional Steelwork
publications@steelconstruct.com
www.steelconstruct.com

ISBN (ECCS): 978-92-9147-133-1
Legal dep.: 408579/16 Printed in Multicomp Lda, Mem Martins, Portugal